ELSEVIER

Colloids and Surfaces
A: Physicochemical and Engineering Aspects 112 (1996) 73–84

COLLOIDS AND SURFACES A

Kinetics of gas hydrate formation in w/o-emulsions The model system trichlorofluoromethane/water/non-ionic surfactant studied by means of dielectric spectroscopy

Thorvald Jakobsen [a], Johan Sjöblom [a,*], Peter Ruoff [b]

[a] *Department of Chemistry, University of Bergen, Allégt. 41, 5007 Bergen, Norway*
[b] *School of Technology and Science, Stavanger College, Box 2557 Ullandhaug, 4004 Stavanger, Norway*

Received 20 December 1995; accepted 25 February 1996

Abstract

The kinetics of trichlorofluoromethane (CCl_3F) hydrate formation in water-in-oil emulsions stabilised by a non-ionic surfactant (Berol 26) were studied by means of dielectric spectroscopy. The dielectric spectra were recorded between 10 MHz and 1 GHz using time domain spectroscopy. A shell model of the dispersed droplets was used to determine the conversion of clathrate hydrate in the emulsion droplets. Simulations of the experimental findings are based on a simple reaction kinetics model. The model consists of three processes: the diffusion of CCl_3F from the continuous oil phase into the dispersed water phase, the slow uncatalysed formation of clathrate hydrate, followed by an autocatalytic production of clathrate hydrate. The overall process is limited by the diffusion of CCl_3F from the continuous oil phase into the dispersed water droplets.

Keywords: Clathrate hydrate; Dielectric spectroscopy; Kinetics; Time domain spectroscopy; Water-in-oil emulsion

1. Introduction

Gas hydrates are clathrate compounds between small gas molecules as guest molecules and water molecules as host molecules. These clathrate hydrates consist of different unit cells which are formed by hydrogen-bonded water. The entrapped guest molecules stabilise the structure by means of van der Waals interactions. Combinations of the different unit cells give rise to structures I, II [1–3] and H [4].

Since the discovery of clathrate hydrates as plugs in gas pipelines [5], there has been an ever-increasing interest to understand and avoid the formation of gas hydrates during the transport of gas. In the beginning of the 1970s clathrate hydrates were identified in deep sea sediments on the east coast of the USA [6,7]. Since these discoveries other findings of clathrate hydrates have been reported in deep sea sediments and in permafrost [8]. Natural clathrate hydrates are mainly formed by methane gas, and the existence of vast deposits indicates significant gas resources.

The development towards total subsea production of oil in the North Sea, results in transportation of unprocessed or minimally processed well fluids to a central processing facility. During this multiphase flow one of the several operational problems that can occur, depending on temperature and pressure, is the formation of gas hydrates. Natural gas- and oil-producers have prevented the gas hydrate formation by thermodynamic means.

* Corresponding author.

PII SO927-7757(96)03578-9

By removing water and maintaining the temperature and pressure at a safe level, or by injecting thermodynamic inhibitors such as glycol or methanol, the equilibrium state is shifted. Recent publications [9–14] show that applications are turning away from thermodynamics to kinetics. Another possibility is the prevention of agglomeration of the clathrate hydrate by adding additives such as polymers and surfactants [10] forming emulsions or microemulsions.

Gas hydrate formation in microemulsions has been studied by several authors [15–18]. It has been found that this gas hydrate formation is dependent on the water-to-surfactant molar ratio which defines the size of the micelles and influences the state of the microaqueous phase. It is observed that gas hydrate particles precipitate from the micelles and are separated from the source of the aqueous phase [19].

Two terms are needed to give a kinetic description of the clathrate hydrate formation: the primary nucleation or the induction time, and the crystal growth. During the induction period, nuclei grow until a critical size is obtained, then crystal growth occurs. Makogen [20] found that the nucleation process was an interfacial phenomenon which was dependent on pressure, temperature and the degree of supercooling. This model does not give a quantitative prediction of the amount of clathrate hydrate formed as a function of time. Lekvam and Ruoff [21] explain the gas hydrate formation in methane hydrate as being an autocatalytic process, where the number of sites for macroscopic growth increases during the induction time until a critical concentration of clathrate hydrate species is reached. Above this critical concentration the autocatalytic reaction predominates, and is limited by the transport of methane gas in water. This model is not only able to describe the induction period relatively correctly, but also shows correct hysteresis behaviour in the formation and melting of methane hydrate [22].

In this work we have studied clathrate hydrate formation in a model water-in-oil emulsion. The reasons for choosing emulsified systems are several. If correctly stabilised, the emulsified system may offer a convenient way to transport the clathrate hydrate and to prevent it from further agglomeration. When comparing water-in-oil emulsions and water-in-oil microemulsions as technical solutions for such a transport, it is obvious that the emulsified system offers better possibilities for keeping down the costs of surfactants during the transport stage. Also, when reaching a separation unit the emulsified system can be more efficiently broken and the components separated. The clathrate hydrate is formed in a water-in-oil emulsion stabilised by a non-ionic surfactant. As a clathrate hydrate-forming species, trichlorofluoromethane (CCl_3F) is used. This molecule gives rise to clathrate hydrate formation under mild conditions (3–7 °C, 1 bar). The clathrate hydrate formation is followed by means of dielectric spectroscopy (time domain spectroscopy (TDS) technique). In this paper it is shown that by means of this technique we can determine formation temperatures, conversion rates and the kinetics of the hydrate formation.

2. Experimental and Methods

2.1. Sample Preparation and Measurement

The emulsions were prepared from doubly distilled water, containing 1 wt.% NaCl (99.5% from Merck AG, Germany) and Exxol D-80. Exxol D-80 is a mixture of aliphatic and cycloaliphatic hydrocarbons with 10–13 carbons (less than 1% aromatics). The commercial surfactant Berol 26, tetraoxyethylene nonyl-phenyl ether (C_9-Ph-EO_4) (99.7% Akzo Nobel AB, Sweden) was used as supplied. CCl_3F (99% from Merck AG, Germany) was used without further purification. Prior to an experiment, a water-in-oil emulsion of Exxol D-80, 1% NaCl-solution and Berol 26 was prepared using an emulsor screen head for 3 min. After mixing, the emulsion was cooled to 3.0 ± 0.1 °C. The water-in-oil emulsion was then transferred to an aluminium cell. The experiment was started when CCl_3F (at 3.0 °C) was added to the emulsion. The emulsion had a 60:40 water-to-oil ratio and the oil phase consisted of Exxol D-80 and CCl_3F. The amount of CCl_3F was varied from 0.80 to 1.20 mol ratio relative to water. The surfactant was added to the oil phase at a concentration of 4 vol.%.

An aluminium cell was used for the studies of

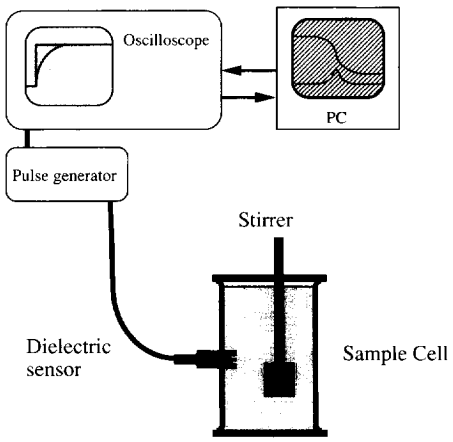

Fig. 1. The experimental set up: the sample cell (175 cm^3) with dielectric sensor, oscilloscope with pulse generator, and a PC for logging and calculation of dielectric spectra.

clathrate hydrate formation. The volume of the cell was 175 cm^3 and the dielectric sensor was placed on the wall in the middle of the cell (Fig. 1). The cell was placed into a thermostatted water bath at $3.0 \pm 0.1\,^{\circ}C$. During experiments the emulsion was held at a constant stirring rate at 3600 rev min^{-1}. The dielectric spectra of the system were recorded every minute for 100–150 min.

2.2. Dielectric Spectroscopy and Dielectric Model Calculations

The dielectric measurements were performed using the TDS technique [23,24]. The method of total reflection was used, which is based on the study of the change in a rapidly rising voltage pulse. The sample is placed at the end of a coaxial cable, and the reflected pulse shapes are monitored by a sampling oscilloscope (Fig. 1). Fourier transformation of incident ($v(t) \rightarrow V(\omega)$) and reflected ($r(t) \rightarrow R(\omega)$) pulse shapes give a reflection coefficient spectrum ($T(\omega) = R(\omega)/V(\omega)$). From transmission line theory, the reflection coefficient spectrum $T(\omega)$ can be expressed as a function of complex permittivity, and the dielectric spectrum $\epsilon^*(\omega) = \epsilon'(\omega) - i\epsilon''(\omega)$ is obtained by solving of the corresponding equation.

A Cole–Cole model function [24]

$$\epsilon^*(\omega) = \frac{\epsilon_s - \epsilon_\infty}{1 + (i\omega\tau)^{1-\alpha}} \tag{1}$$

was fitted to the experimental points. Here ϵ_s is the static permittivity, ϵ_∞ the permittivity at high frequencies, ω is the angular frequency and τ is the relaxation time.

In these experiments a Hewlett Packard digitising oscilloscope (HP54120B) and a pulse generator (HP54123A) were used. The reflected pulse was observed in a time window of 100 ns, and the pulses were Fourier-transformed at 150 frequencies from 10 MHz to 1 GHz. The reference solutions ethanol, pentanol and dichloromethane were used for calibration. A personal computer was used for controlling the measuring cycles, which also performed the necessary calculations.

The present work shows that gas hydrate formation in water-in-oil emulsions can be followed by means of the TDS technique. The build-up of clathrate hydrate structures owing to water conversion can be monitored dielectrically as a function of time, and calculations from permittivity to concentration can give us the reaction rate. Permittivities are transformed to concentration according to a model where we assume that the CCl_3F hydrate formation starts at the droplet interface, and the CCl_3F hydrate grows in the droplets, forming a shell around the emulsion droplet with fixed permittivity. We employ the dielectric shell model initially proposed by Hanai et al. [25] in order to explain the conversion of water. In this model a shell is included in the dispersed droplets, which have different dielectric properties from the core (the rest of the disperse droplet) and the continuous phase.

The complex permittivity (ϵ^*) of the emulsion droplets with radius R, having equivalent homogeneous permittivity ϵ_p^* and surrounded by a continuous medium of ϵ_a^*, is given by

$$\left(\frac{\epsilon^* - \epsilon_p^*}{\epsilon_a^* - \epsilon_p^*}\right)\left(\frac{\epsilon_a^*}{\epsilon^*}\right)^{1/3} = 1 - \phi \tag{2}$$

where ϕ is the volume fraction of dispersed phase. The permittivity of the dispersed droplet ϵ_p^* is a

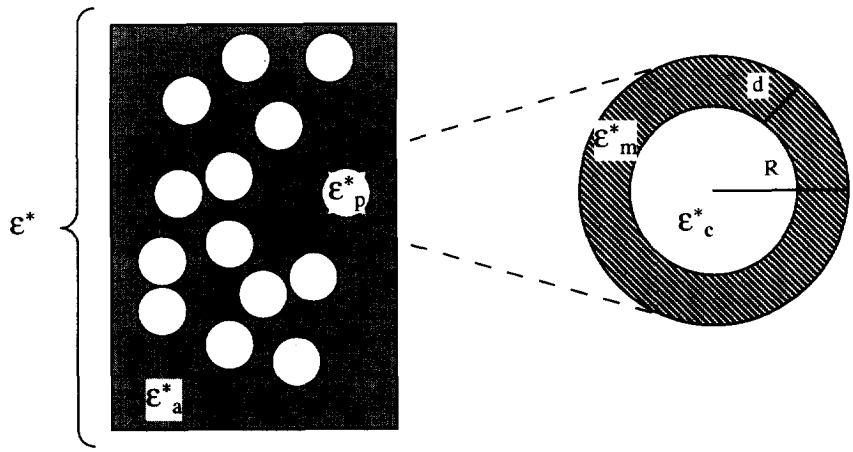

Fig. 2. Sketch of the shell model used to calculate the water conversion (mol) from permittivities. The complex permittivity (ϵ^*) is given by Eq. (2), where ϵ_p^* is the permittivity of the dispersed droplets with radius R surrounded by a continuous medium ϵ_a^*. The permittivity of the dispersed droplet ϵ_p^* is given by Eq. (3) and is a function of the core (ϵ_c^*) and the shell (ϵ_m^*).

parameter which is calculated by the equation

$$\epsilon_p^* = \epsilon_m^* \frac{2(1-v)+(1+2v)E}{2+v+(1-v)E} \quad (3)$$

with $E = \epsilon_c^*/\epsilon_m^*$ and $v = (1-d/R)^3$. Here ϵ_c^* is the permittivity of the core, and ϵ_m^* is the permittivity of the shell around the core as shown in Fig. 2, which defines all parameters.

By inserting dielectric parameters of the continuous phase, the dispersed phase (water) and the shell (CCl_3F hydrate), we can solve the model spectra for the emulsion system for a different relative thicknesses of the shell (d/R). A model spectrum based on Eqs. (2) and (3) is shown in Fig. 3. The spectrum is based on a shell-thickness ratio (d/R) of 0.1, and the dielectric parameters used are given in Table 1.

According to the literature gas hydrates with structure II have a static permittivity (ϵ_s) of 56, permittivity at high frequency (ϵ_∞) of 4.5 and relaxation time (τ) 1×10^{-6} s [26] as shown in Table 1. The dispersion owing to CCl_3F hydrate is in the low frequency region (Fig. 3). In the high frequency region there is a dispersion owing to free water and the ethoxy groups in the surfactant. The dispersion of the ethoxy group is not taken into account in the present model. The frequency region investigated is from 10 MHz to 1 GHz (marked in Fig. 3), and shows a dispersion which is due to the polarisation inside the emulsion water droplets. In this frequency region we find information about the changes in the emulsion system and observe the formation of clathrate hydrate.

A more realistic hydrate model would involve a gradual increase of the permittivity from a value of 4.5 (completely covered with gas hydrate) to a

Table 1
Dielectric values used in the calculation of the shell model

Medium	Static permittivity (low frequency) ϵ_s	Permittivity at optical frequency, ϵ_∞	Relaxation time, τ	Sigma, σ (Sm)
Water	86.5	5.6	15 ps	1.5
Oil	2.0	2.0	0	0
CCl_3F	2.0	2.0	0	0
CCl_3F hydrate	58.0	4.5	5 μs	0
Emulsion	26.0	15.0	≈1 ns	0

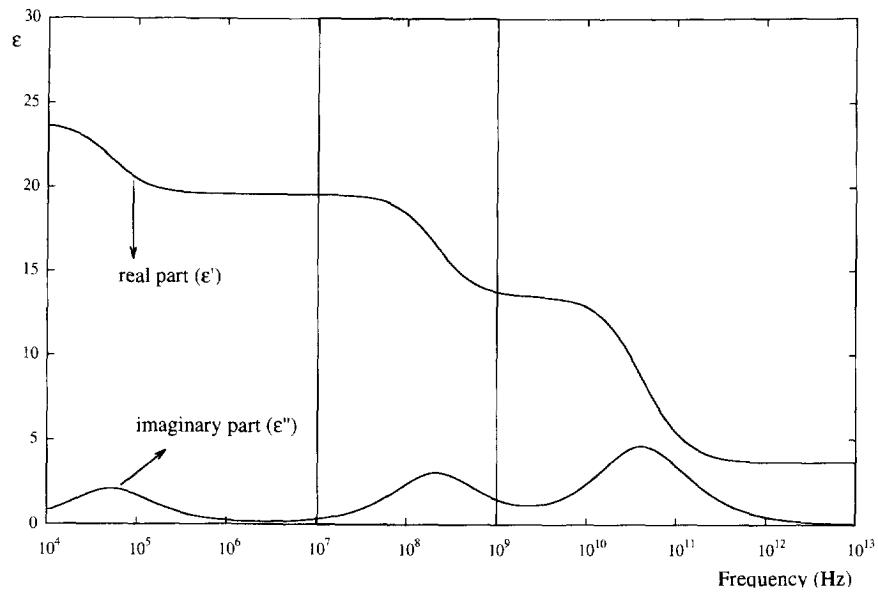

Fig. 3. Model spectrum based on Eqs. (2) and (3) with a shell thickness ratio (d/R) of 0.10. The frequency region investigated in the experiments is from 100 MHz (10^7) to 1 GHz (10^9) marked by the vertical lines in the figure. The first dispersion is due to the gas hydrate, the second dispersion is due to the Maxwell–Wagner–Sillars effect and the last dispersion is due to the water relaxation. The figure shows that the investigated frequency region gives dielectric information about the changes in the system during gas hydrate formation.

permittivity of 86 (free water at 3°C) in the dispersed droplets. An extension of the model of Hanai et al. [25] with several shells of varying dielectric properties has been used by Asami and Irimajiri [27]. This model provides a gradual change of permittivity to be modelled and gives a theoretically better interpretation. However, since our model system and its dielectric properties are rather difficult to interpret in detail, we have chosen to adopt a simpler two-state model for our data.

2.3. Mechanistic Model and Model Computations

The reaction model consists of three processes, which define the reactants (CCl_3F and H_2O) and the CCl_3F hydrate H:

$$CCl_3F_{(oil)} \underset{k_2}{\overset{k_1}{\rightleftharpoons}} CCl_3F_{(aq)} \quad (4)$$

$$CCl_3F_{(aq)} + 17H_2O \xrightarrow{k_3} H \quad (5)$$

$$CCl_3F_{(aq)} + 17H_2O \underset{k_5}{\overset{k_4[H]}{\rightleftharpoons}} H \quad (6)$$

Eq. (4) describes the diffusion of CCl_3F from the oil phase into the emulsion droplet. Eq. (5) illustrates a slow formation of clathrate hydrate based on the assumption that a clathrate unit cell of type II is formed [4,26] although Davidson and Ripmeester [28] describe the CCl_3F hydrate as slightly nonstoichiometric. Eq. (6) [21] gives the autocatalytic formation of CCl_3F hydrates from CCl_3F and H_2O.

Computations of the reaction model were performed by integrating the rate equations shown in Eqs. 4–6 with the FORTRAN subroutine LSODE [29]. The calculation was performed with a Macintosh LC 475.

3. Results and Discussion

3.1. Clathrate hydrate formation temperature

At 4.2 ± 0.1°C the clathrate hydrate formation starts in the emulsified system after 20 min. This was found by a temperature scan of the system

from 10°C with temperature steps of 0.5 ± 0.1°C and a delay of 30 min at each interval. If the temperature is lowered to 3.0 ± 0.1°C, the onset of gas hydrate formation is spontaneous. The equilibrium temperature of CCl_3F hydrate is 8.4°C [30] at 1 bar, but the experiments show that no CCl_3F hydrates are formed at this temperature, not even after 5 h of constant stirring.

The CCl_3F hydrate formation in emulsions requires a $\Delta T \approx 5.3$°C (8.4°C − (3.0 ± 0.1°C)). The reason for the low hydrate formation temperature may be explained by changes in the equilibrium temperature owing to freezing-point depression and the effect of supercooling in emulsions. The presence of sodium chloride in the aqueous phase will lower the equilibrium temperature of CCl_3F hydrate formation. Experiments show that a sodium chloride concentration of 3% totally inhibits the CCl_3F hydrate formation, while a concentration below 2% does not. Makogen [20] and Vysniauskas and Bishnoi [31] reported supercooling ($\Delta T \approx 2$°C) for methane and ethane hydrates. The reason for the higher degree of supercooling in our system may be analogous to the freezing of water-in-oil emulsions, which requires a supercooling owing to the fact that small liquid droplets can undergo large supercooling while bulk samples do not supercool more than a few degrees [32,33]. The large degree of supercooling might be reduced by use of a longer delay at each temperature interval (more than 30 min) and higher mechanical energy added to the system (higher activation energy).

The melting temperature of the CCl_3F hydrate in water-in-oil emulsions is determined to be 4.4 ± 0.1°C. After increasing the temperature to 7°C, melting the clathrate hydrate, and then decreasing the temperature, the formation starts immediately at 4.4 ± 0.1°C. This indicates that hydrate precursors exist in the system [20,34]. Our temperature scan experiments cannot verify a hysteresis behaviour which a study by Lekvam and Ruoff confirms [22]. However, the fact that the spontaneous clathrate hydrate formation temperature is increased with about 1.4°C, indicates that existing precursors in the system influence the formation temperature or the degree of supercooling.

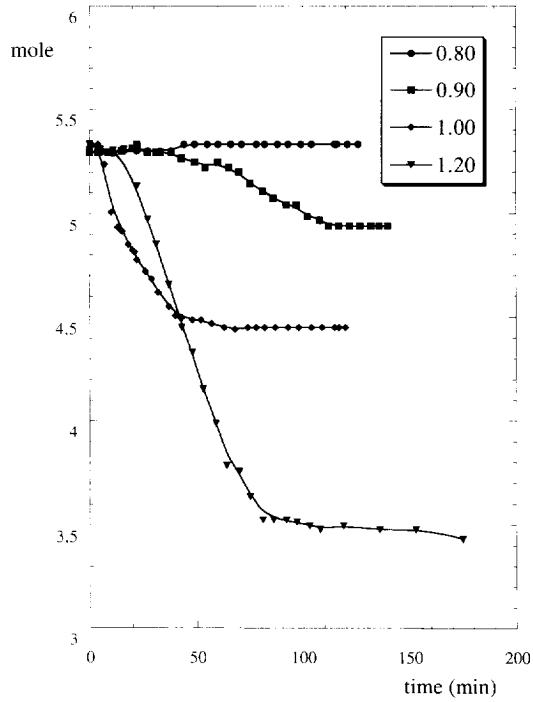

Fig. 4. Static permittivity as a function of time during gas hydrate formation. The mole ratio of CCl_3F:H_2O is 0.80, 0.90, 1.00 and 1.20.

3.2. Dielectric Properties of the system

Fig. 4 shows the static permittivity (ϵ_s) as a function of time after addition of different amounts of CCl_3F to the emulsion. The mole ratio of CCl_3F to water used in these experiments were 0.80, 0.90, 1.0 and 1.2, based on the assumption that a clathrate unit cell of type II is formed [4,26]. The results show that the static permittivity (ϵ_s) starts at a level determined by the water content in the emulsion and decreases to a final level which depends on the final amount of water molecules converted to gas hydrates. The degree of water conversion depends on the ratio of $CCl_3F : H_2O$.

An example of a dielectric spectrum of CCl_3F hydrates in the water-in-oil emulsion is shown in Fig. 5. In the same figure a Cole–Cole model fitting is presented and a dielectric dispersion is observed in the frequency region investigated. The Cole–Cole model accounts for a situation where the dielectric relaxation is ascribed to a polarisation inside the dispersed droplets, allowing a cer-

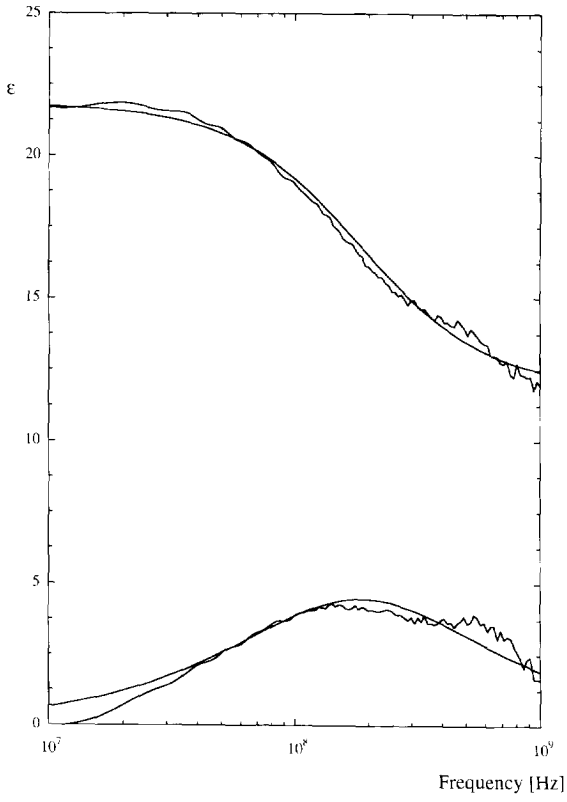

Fig. 5. An example of a dielectric spectrum of gas hydrate in a water-in-oil emulsion. In the same figure a Cole–Cole model fitting (Eq. (1)) is shown.

tain degree of polydispersity. The changes in the dielectric parameters due to CCl_3F hydrate formation are shown in Figs. 6a–6c. These results cover an experiment where the mole ratio $CCl_3F:H_2O$ was 1.20, and the data are fitted to a Cole–Cole function (Eq. (1)).

The static permittivity (ϵ_s) and the permittivity at high frequency (ϵ_∞) show the same dependence on CCl_3F hydrate formation (Fig. 6a). Model calculations and experiments show that the difference between permittivity of CCl_3F and Exxol D-80 has little influence on the complex permittivity when CCl_3F is replaced by Exxol D-80. The dielectric parameters observed are therefore due to the changes in the dispersed and continuous phases as the CCl_3F hydrate formation sets in.

The relaxation modes in these studies are due to the Maxwell–Wagner–Sillars effect [35–37]. The relaxation time (τ) in the experiments decreases from about 1000 ± 100 ps, to a final level of 200 ± 20 ps during the CCl_3F hydrate formation (Fig. 6b). The relaxation times show that during the formation of CCl_3F hydrates there will be an increasing sodium chloride concentration in the free water as the rest of the water becomes bound into the gas hydrate lattice. The experimental value of relaxation time of 200 ps corresponds to a 3% (w/v). NaCl solution, which is a high enough electrolyte concentration to give a thermodynamic inhibition of gas hydrate formation.

The distribution factor (α) increases from 0.05 ± 0.03 to 0.30 ± 0.01 during the gas hydrate formation (Fig. 6c). This is due to increased polydispersity inside the dispersed droplet owing to the CCl_3F hydrate. The gas hydrate structure is assumed to influence the mobility of water and thus give a more structured state of the free water. This situation is similar to that of thawed ice or cold water, which both have a tendency to retain a more structured state owing to lower molecular activity. This results in partly bound water which decreases the relaxation time. The reduced relaxation time owing to partly bound water may be detected in the frequency region investigated and contributes to the increased distribution factor.

3.3. Kinetics and computations of the mechanistic models

Fig. 7a shows a simulation of an experiment where water is consumed owing to the formation of clathrate hydrate. The mole ratio $CCl_3F:H_2O$ is 1.20.

Fig. 7b gives the concentration of CCl_3F in the dispersed water phase, where CCl_3F is diffusing from the oil phase into the water phase (Eq. (4)). The first two points in the simulation show the increasing amount of CCl_3F in the water phase. The slow reaction between $CCl_3F_{(aq.)}$ and H_2O-forming CCl_3F hydrate (H) (Eq. (5)) starts when the concentration of $CCl_3F_{(aq.)}$ has reached a certain value, leading to a slow consumption of $CCl_3F_{(aq.)}$. This can be seen from the next points in the simulation. When the CCl_3F hydrate species (H) have reached a critical amount, the autocatalytic reaction starts and the total process is dominated by Eq. (6). The autocatalytic reaction

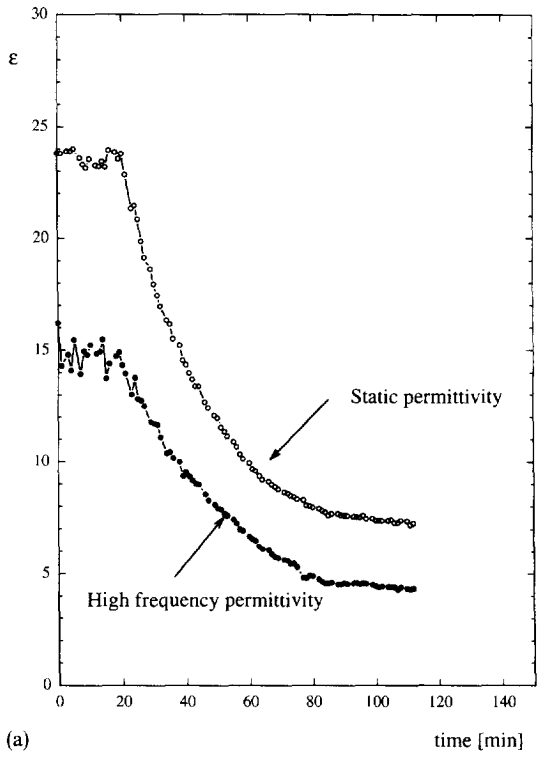

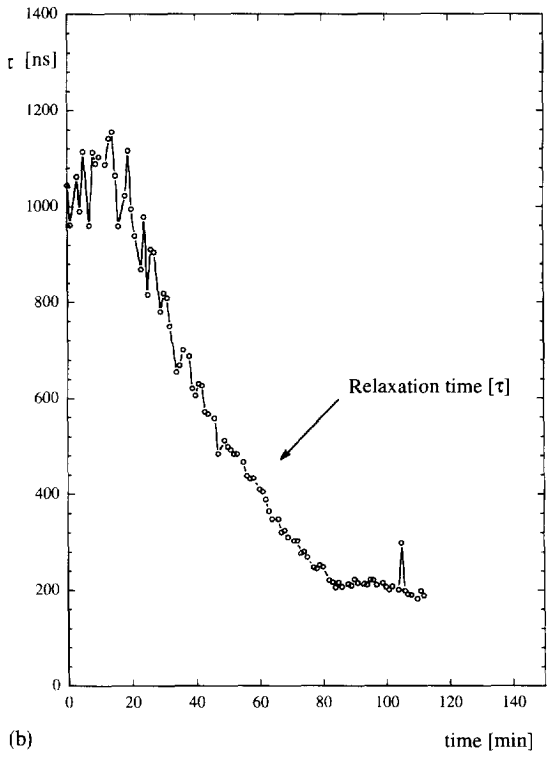

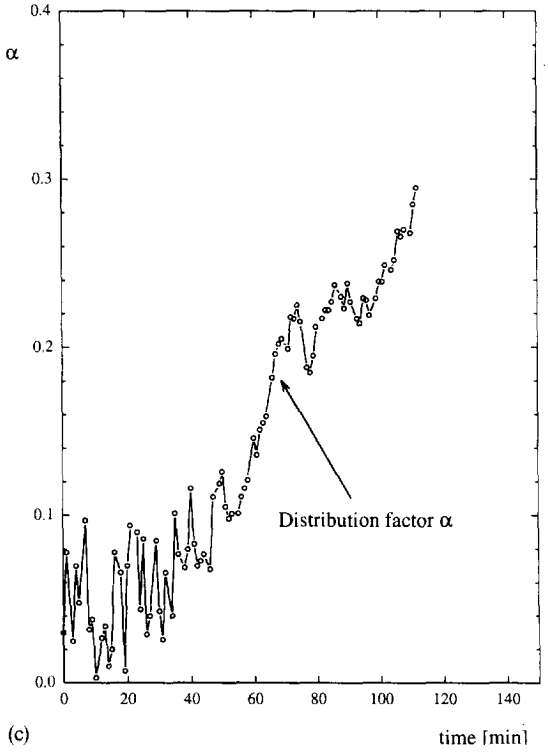

Fig. 6. Results from an experiment with mole ratio $CCl_3F:H_2O = 1.20$. Fig. 6a shows the static permittivity (ϵ_s) and permittivity at high frequency (ϵ_∞) as a function of time. Figs. 6b and 6c show the relaxation time (τ) and distribution factor (α) respectively as a function of time.

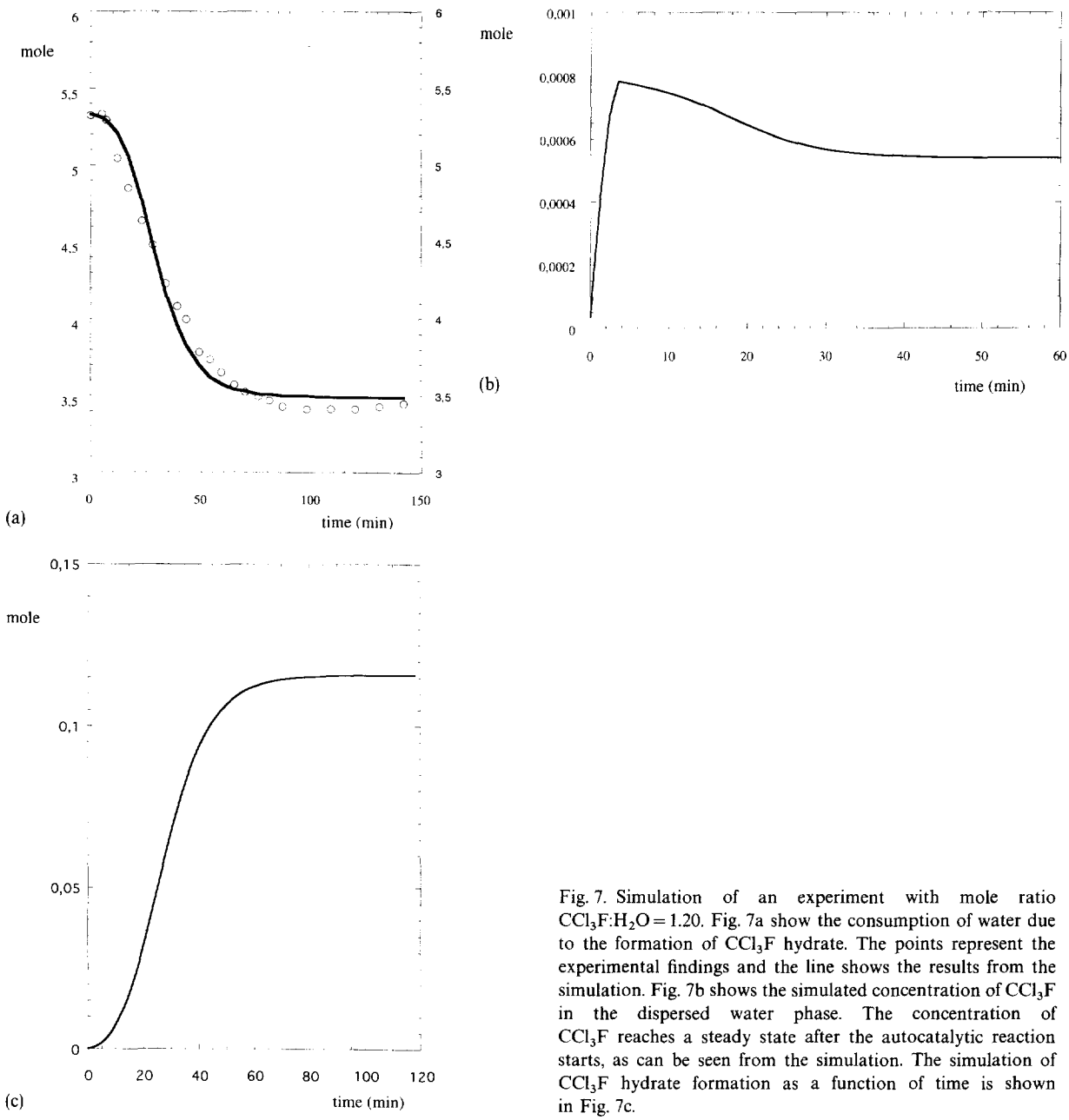

Fig. 7. Simulation of an experiment with mole ratio $CCl_3F:H_2O = 1.20$. Fig. 7a show the consumption of water due to the formation of CCl_3F hydrate. The points represent the experimental findings and the line shows the results from the simulation. Fig. 7b shows the simulated concentration of CCl_3F in the dispersed water phase. The concentration of CCl_3F reaches a steady state after the autocatalytic reaction starts, as can be seen from the simulation. The simulation of CCl_3F hydrate formation as a function of time is shown in Fig. 7c.

increases the consumption of $CCl_3F_{(aq.)}$. As a consequence, the concentration of CCl_3F decreases and reaches a steady state (Fig. 7b).

The formation of clathrate hydrates (H) is shown in Fig. 7c. The evolution in this curve is in agreement with the consumption of water as shown in Eqs. (4)–(6).

Results from the fittings of the rate constants to the experimental points for the different experiments (mole ratio $CCl_3F:H_2O = 0.80–1.20$) are presented in Table 2.

k_1 and k_2 are the rate constants of the first process (Eq. (4)) which is the diffusion of CCl_3F from the continuous oil phase into the dispersed

Table 2
Rate constant values obtained in the model calculations of rate equations

Rate constant	Mole ratio $CCl_3F:H_2O$			
	0.80	0.90	1.0	1.20
k_1 (min^{-1})	0.098	0.080	0.098	0.100
k_2 (min^{-1})	47	50	47	47
k_3 ($M^{-l}\ min^{-1}$)	0.400	0.019	0.360	0.042
k_4 ($M^{-l}\ min^{-1}$)	115	154	115	84
k_5 (min^{-1})	0.290	0.312	0.290	0.164

l is the reaction order used in the experiments.

water phase. The diffusion is dependent on the contact frequency between the molecules in the continuous and dispersed phase, the solubility properties of the species, the size of the diffusing species and the surfactant. The contact frequency between the reacting species is high owing to the high volume fraction of disperse phase and the vigorous stirring, and is not expected to be the limiting element in k_1 and k_2. CCl_3F is soluble in the model oil and has a low solubility in the aqueous phase as can be seen from the low concentration of CCl_3F inside the emulsion droplet (Fig. 7c). The surfactant membrane acts as the diffusion barrier and this barrier depends on the hydrophilic/hydrophobic properties of the surfactant, the concentration of the surfactant, the hydrophobic property of the oil phase, and the hydrophilic property of the aqueous phase. From Fig. 7b it can be seen that the CCl_3F concentration in the water phase is very low after the autocatalytic reaction has started, and it is obvious that the diffusion through the interfacial membrane appears to be the rate-limiting step in the overall process.

The second process (Eq. (5)) is the slow (uncatalysed) formation of clathrate hydrates H. The model used in this work is based on the work of Lekvam and Ruoff [21] where they describe the induction period as part of an autocatalytic process. This model is able to describe the induction period relatively correctly. Barrer and Ruzicka [38] and Barrer and Edge [39] found that methane and krypton hydrates show an induction time, while ethane, ethylene and cabondioxide hydrate do not give induction times. In some of our experiments we observed an induction time, while Cheng and Pinder [40] and Cady [41] have shown that CCl_3F hydrate does not show induction time. Vysniauskas and Bishnoi [31] proposed a semi-empirical model, where the initial rate is an explicit function of the interfacial area of gas to water, the degree of super cooling, the activation energy, and the total gas pressure. The observed induction time may be due to elements which Vysniauskas and Bishnoi describe: insufficient supercooling, a reduced contact frequency between the reacting species, energy added to the system (stirring), and an inhomogeneous mixture of the viscous emulsion and low viscous CCl_3F. The cooled, concentrated emulsions are very viscous and the addition of the low viscous CCl_3F results in a inhomogeneous mixture during the first minutes of the experiment. These conditions lead to a less well-defined contact frequency between the reacting species, and may delay the spontaneous clathrate hydrate formation leading to a fictive induction time. In addition the highly viscous emulsions, combined with a high mixing speed, will give a slight increase in temperature and may result in insufficient supercooling, which also may delay the spontaneous clathrate hydrate formation. Owing to these facts and to the complexity of the emulsified system, we use a simplified model where the rate constant k_3 contains stochastic elements as described above.

The third process (Eq. (6)) quantified by k_4 and k_5, is the autocatalytic formation of CCl_3F hydrates (the growth phase). After the slow build-up of clathrate hydrate particles to a critical concentration (Eq. (5)), Eq. (6) is responsible for the main conversion of CCl_3F hydrate. The formation is now limited by the diffusion of CCl_3F from the oil phase into the water phase. This conclusion is analogous to the conclusion by Skovborg and Rasmussen [42] and Lekvam and Ruoff [21] who proposed a model based on the assumption that the transport of the gas molecules from gas phase to liquid phase is the rate-determining step in the overall hydrate-formation process, when describing water/gas systems. The model of Skovborg and Rasmussen gives no quantitative predictions of the amount of gas hydrate formed as a function of time. The model by Lekvam and Ruoff corrects

for this and also gives the correct hysteresis behaviour in the formation and melting of methane hydrates [22].

The validity of the quantities of gas hydrates formed, and the conversion of water found in our experiments should also be discussed. The model used to calculate the amount of gas hydrates or converted water is simplified. The model assumes a shell with a distinct separation of the gas hydrate (the shell) from the water phase (the core), although it would be more natural to assume a mixture in the dispersed phase. Even though we use a simple model on a complex system, the static permittivity in the frequency region investigated is a good indication of the final amount of free water. This is because the static permittivity of the other constituents has a relatively equal and low value as compared to water. The amount of water converted is confirmed by the increased NaCl concentration in the free water, determined by the relaxation time. Although the relaxation time is most likely influenced by partly structured water and by gas hydrates as shown by the increased distribution factor, the level of relaxation times reveals some details of the conversion process.

Another factor is the transition from "slush"-hydrates (with about 60% "free" water) to "powder"-hydrates (about 10% "free" water). This transition is an ageing effect. The "slush"-hydrates behave like dispersions with a possibility to flow, while "powder"-hydrates appear as solid plugs. When storing the samples for several days, it is visually observed that gas hydrates formed in stable emulsions show a much longer ageing time from "slush"- to "powder"-hydrate than gas hydrate in a conventional three phase system. By choosing a proper surfactant it can be possible to limit or inhibit the gas hydrate formation. The ageing effect may be delayed by formation of stable emulsions and this effect can avoid plugs in tubing by keeping the gas hydrate in a dispersed state when submitted to flow.

Acknowledgements

Industrial support from Elf Petroleum, Saga and Statoil is greatly appreciated. Thorvald Jakobsen would like to thank the Norwegian Research Council (NFR) for a Dr. Scient. grant. The dielectric instrumentation was financed by the NFR and the University of Bergen.

References

[1] M. von Stackelberg, Naturwissenchaften, 11 (1949) 327.
[2] M. von Stackelberg and H.R. Müller, Z. Elektrochem., 58 (1954) 25.
[3] M. von Stackelberg and W. Jahns, Z. Elektrochem., 58 (1954) 162.
[4] J.A. Ripmeester, J.S. Tse, C.I. Ratcliffe and B.M. Powell, Nature, 325 (1987) 135.
[5] E.G. Hammerschmidt, Ind. Eng. Chem., 26 (1934) 851.
[6] D.L. Katz, J. Pet. Technol., 23 (1971) 419.
[7] C. Bily and J.W.L. Dick, Bull. Can. Pet. Geol., 22 (1974) 340.
[8] K.A. Kvenvolden, Chem. Geol., 71 (1988) 41.
[9] E.D. Sloan and F. Fleyfel, AIChE J., 37 (1991) 1281.
[10] B. Mueller-Bongartz, T.R. Wildeman and E.D. Sloan, A hypothesis for hydrate nucleation phenomena, 2nd. Int. Offshore and Polar Eng. Conf., 14–19 June 1992, San Francisco, USA.
[11] A.R. Nerheim, T.M. Svartaas and E.K. Samuelsen, Investigation of hydrate kinetics in the nucleation and early growth phase by laser light scattering, 2nd Int. Offshore and Polar Eng. Conf., 14–19 June 1992, San Francisco, USA.
[12] P. Englezos, Trans. Inst. Chem. Eng., 70 (1992) 43.
[13] P. Englezos and Y.T. Ngan, Fluid Phase Equilibria, 92 (1994) 271.
[14] O. Urdahl, A. Lund, P. Mørk and T.-N. Nilsen, Chem. Eng. Sci., 50 (1995) 863.
[15] J.L. Fulton, J.P. Blitz, J.M. Tingey and R.D. Smith, J. Phys. Chem., 93 (1989) 4198.
[16] H. Nguyen, J.B. Phillips and V.T. John, J. Phys. Chem., 93 (1989) 8123.
[17] H.T. Nguyen, N. Kommareddi and V.T. John, J. Colloid Interface Sci., 155 (1993) 482.
[18] H. Førdedal, Ø. Holt and J. Sjöblom, J. Disp. Sci. Technol., 15 (1994) 465.
[19] V.T. John, N.S. Kommareddi, M.S. Ayyagari, M. Tata, F. Kaeayigitoglu, G.L. McPherson, in E.D. Sloan, J. Happel and M.A. Hnatow (Eds.), New Directions in Hydrate Technology, International Conference on Natural Gas Hydrate, Annals of the New York Academy of Science, New York, 1993.
[20] Y.F. Makogen, Hydrates of Natural Gas, PennWell, Tulsa, 1981.
[21] K. Lekvam and P. Ruoff, J. Am. Chem. Soc., 115 (1993) 8565.
[22] K. Lekvam and P. Ruoff, Int. J. Chem. Kinet., submitted for publication.

[23] R.H. Cole, Ann. Rev. Phys. Chem., 28 (1977) 283.
[24] R.H. Cole, J.G. Berberian, S. Mashimo, G. Chryssikos, A. Burns and E. Tombari, J. Appl. Phys., 66 (1989) 793.
[25] T. Hanai, K. Asami and N. Koizumi, Bull. Inst. Chem. Res., 57 (1979) 197.
[26] D.W. Davidson, in F. Franks (Ed.), Water a Comprehensive Treatise, Vol. 2, Plenum Press, New York, 1973.
[27] K. Asami and A. Irimajiri, Biochimica et Biophysica Acta., 778 (1984) 570.
[28] D.W. Davidson and J.A. Ripmeester, in J.L. Atwood, J.E.D. Davies and D.D. MacNicol (Eds.), Inclusion Compounds, Vol. 3, Physical Properties and Applications, Academic Press, London, 1984.
[29] A.C. Hindmarsh, ACM-SIGNUM Newslett., 15 (1980) 10.
[30] T.A. Wittstruck, W.S. Brey, A.M. Buswell and W.H. Rodebush, J. Chem. Eng. Data, 6 (1961) 343.
[31] A. Vysniauskas and P.R. Bishnoi, Chem. Eng. Sci., 40 (1985) 299.
[32] I.D. Chapman, J. Phys. Chem., 72 (1968) 33.
[33] M. Clausse, in P. Becher (Ed.), Encyclopedia of Emulsion Technology, Basic Theory, Vol. 1, M Dekker, New York, 1983.
[34] A. Vysniauskas and P.R. Bishnoi, Chem. Eng. Sci., 38 (1983) 1061.
[35] J.C. Maxwell, A Treatise on Electricity and Magnetism, Clarendon Press, Oxford, 1892.
[36] K.W. Wagner, Arch. Electrotech., 3 (1914) 100.
[37] R.W. Sillars, Proc. Inst. Electr. Eng. London, 80 (1937) 378.
[38] R.M. Barrer and D.J. Ruzicka, Trans. Faraday Soc., 58 (1962) 2262.
[39] R.M. Barrer and A.V.J. Edge, Proc. R. Soc., 300 (1967) 1.
[40] W.K. Cheng and K.L. Pinder, Can. J. Chem. Eng., 54 (1976) 377.
[41] G.H. Cady, J. Phys. Chem., 87 (1983) 4437.
[42] P. Skovborg and P. Rasmussen, Chem. Eng. Sci., 49 (1994) 1131.